Identification of Live Germ-Cell Desquamation as a Major Mechanism of Seasonal Testis Regression in Mammals: A Study in the Iberian Mole (Talpa occidentalis) 1

Authors: Dadhich, Rajesh K., Barrionuevo, Francisco J., Real, Francisca M., Lupiañez, Darío G., Ortega, Esperanza, et al.

Source: Biology of Reproduction, 88(4)

Published By: Society for the Study of Reproduction

URL: https://doi.org/10.1095/biolreprod.112.106708

BIOLOGY OF REPRODUCTION (2013) **88**(4):101, 1–12
Published online before print 20 March 2013.
DOI 10.1095/biolreprod.112.106708

Identification of Live Germ-Cell Desquamation as a Major Mechanism of Seasonal Testis Regression in Mammals: A Study in the Iberian Mole (*Talpa occidentalis*)[1]

Rajesh K. Dadhich,[3,4] Francisco J. Barrionuevo,[3] Francisca M. Real, Darío G. Lupiañez,[5] Esperanza Ortega,[6] Miguel Burgos, and Rafael Jiménez[2]

Departamento de Genética, Instituto de Biotecnología, Universidad de Granada, Granada, Spain

ABSTRACT

In males of seasonally breeding species, testes undergo a severe involution at the end of the breeding season, with a major volume decrease due to massive germ-cell depletion associated with photoperiod-dependent reduced levels of testosterone and gonadotropins. Although it has been repeatedly suggested that apoptosis is the principal effector of testicular regression in vertebrates, recent studies do not support this hypothesis in some mammals. The purpose of our work is to discover alternative mechanisms of testis regression in these species. In this paper, we have performed a morphological, hormonal, ultrastructural, molecular, and functional study of the mechanism of testicular regression and the role that cell junctions play in the cell-content dynamics of the testis of the Iberian mole, *Talpa occidentalis*, throughout the seasonal breeding cycle. Desquamation of live, nonapoptotic germ cells has been identified here as a new mechanism for seasonal testis involution in mammals, indicating that testis regression is regulated by modulating the expression and distribution of the cell-adhesion molecules in the seminiferous epithelium. During this process, which is mediated by low intratesticular testosterone levels, Sertoli cells lose their nursing and supporting function, as well as the impermeability of the blood-testis barrier. Our results contradict the current paradigm that apoptosis is the major testis regression effector in vertebrates, as it is clearly not true in all mammals. The new testis regression mechanism described here for the mole could then be generalized to other mammalian species. Available data from some previously studied mammals should be reevaluated.

germ-cell apoptosis, germ-cell desquamation, mammals, seasonal breeding, testis regression

INTRODUCTION

The germinative epithelium of the testis, the tissue where male gametes are produced, is located inside the seminiferous tubules and composed of somatic (Sertoli) and germ cells. Spermatogonia, preleptotene spermatocytes, and the nuclei of Sertoli cells (which are epithelial cells) occupy basal positions, whereas the rest of meiotic and postmeiotic germ cells fill the whole depth of the epithelium. Sertoli cells have the role of supporting, nursing, and regulating germ-cell function, permitting them to migrate from basal to apical positions as meiosis and spermiation proceed.

In continually, nonseasonally breeding animals, a hormonally controlled equilibrium is established between apoptosis, cell proliferation, and meiosis initiation that maintains the relative numbers of all these germ cell types at constant levels throughout the animal's life [1, 2]. However, seasonal breeders do not require gametes during the nonbreeding season, so that sperm production is halted. As a consequence, testis volume decreases considerably during this period, because of the absence of most meiotic and postmeiotic cell types in the germinative epithelium. This process coincides with low testosterone production by the testis, which is in turn a direct consequence of substantial decrease in the serum concentration of gonadotropic hormones, generally derived from photoperiod-mediated regulation [3].

Cell junctions are important in the regulation of spermatogenesis. Sertoli cells form the so-called blood-testis barrier (BTB), a testis-specific, modified occluding junction, which is constituted by Sertoli-Sertoli cell-tight junctions with ectoplasmic specializations (ES) located at the basal third of the seminiferous epithelium [4–7]. The BTB thus separates two compartments in the seminiferous epithelium: the basal compartment, which contains spermatogonia, preleptotene, and leptotene spermatocytes; and the adluminal one, which contains most meiotic and postmeiotic cells [4]. This barrier has three main functions: 1) to create a specialized environment; 2) to regulate the passage of molecules; and 3) to serve as an immunological barrier. At the apical pole of Sertoli cells a less complex barrier also forms, containing ES (the so-called apical ES), which retains elongated spermatids and precludes them from falling into the lumen [8]. It is well known that the levels of intratesticular testosterone influence cell-junction assembly. Androgen-suppression experiments have shown that anchoring-junction restructuring in the rat testis leads to germ-cell loss from the seminiferous epithelium [9, 10]. This suggests that a rapid reduction in the intratesticular testosterone levels could be an active mechanism to induce rapid germ-cell depletion in the regressing testes of seasonal breeders.

[1]Supported by Junta de Andalucía through Group PAI BIO-109 and grant P06-CVI-2057, and the Spanish Dirección General de Investigación through grants CGL2004-00863/BOS and CGL-2008-0928/BOS. R.K.D. received a Ph.D. fellowship of the Agencia Española de Cooperación Internacional, Ministerio de Asuntos Exteriores (MAE-AECI).
[2]Correspondence: Rafael Jiménez, Departamento de Genética e Instituto de Biotecnología, Universidad de Granada, Laboratorio 127 CIBM, Centro de Investigación Biomédica, Avenida del Conocimiento 18100 Armilla, Granada, Spain. E-mail: rjimenez@ugr.es
[3]These authors contributed equally to this work.
[4]Current address: Institute of Experimental and Clinical Research (IREC), University of Louvain Medical School, Louvain, Belgium.
[5]Current address: Max Planck Institute for Molecular Genetics, Berlin, Germany.
[6]Current address: Departamento de Bioquímica y Biología Molecular III e Inmunología, Facultad de Medicina, Universidad de Granada, Granada, Spain.

Received: 10 December 2012.
First decision: 17 January 2013.
Accepted: 14 March 2013.

eISSN: 1529-7268 http://www.biolreprod.org
ISSN: 0006-3363

The cell-content dynamics of the seminiferous epithelium has been studied in several seasonally and nonseasonally breeding mammals. In most cases, the role that both apoptosis and cell proliferation play in this process was investigated. Whereas it has been suggested that apoptosis contributes to testicular regression in hamsters [11, 12], white-footed mice [13], and the European brown hare [14], among others, more recent studies have shown that apoptosis is not the cause of the massive germ-cell depletion in the roe deer [15] or the Iberian mole [16]. Thus, the mechanism underlying such a germ-cell depletion remains unknown. We have previously suggested that, alternatively to apoptosis, cell-junction disassembly could be a mechanism in seasonal breeders for late spermatocytes and spermatids to be rapidly eliminated by desquamation within the lumen [16].

The sexual dynamics of the Iberian mole, *Talpa occidentalis*, have been studied in our laboratory over the past 20 yr. The presence of ovotestes (gonads with both ovarian and testicular tissue) in all females is the most intriguing peculiarity of the reproductive biology of this species [17–20], a trait that has also been described in several other mole species [21–23]. The spatiotemporal pattern of testis organogenesis has also been investigated [24] in this strict seasonal breeder [25, 26]. In adult male moles, the nonapoptotic, massive germ-cell depletion occurring during mole testis regression is followed by a wave of spermatogonial cell proliferation that appears to restore the number of spermatogonia lost during the period of spermatogenic inactivity [16]. Thus, current knowledge concerning the reproductive biology of *T. occidentalis*, together with the methods we have developed specifically for managing wild moles, renders this species an excellent model to study the control of seasonal testis variation in the wild.

MATERIALS AND METHODS

Animals and Tissue Preparation

Males of the Iberian mole, *T. occidentalis*, were captured alive in Santa Fe and in Chauchina (Granada province, southern Spain) as described previously [19]. Captures were made with the permission of the Andalusian Environmental Council, and animals were handled following the guidelines and approval of the Ethical Committee for Animal Experimentation of the University of Granada. A dental-wear index was calculated for each animal in order to estimate its age, as described previously [17], to ensure that only adult males were included in this study. Animals were dissected and the testes were removed under sterile conditions. In most cases, the two testes of each animal were isolated, weighed, and one of them, together with the annexed epididymis, was fixed overnight in a 50× volume of 4% paraformaldehyde at 4°C and then embedded in paraffin according to standard procedures, whereas the other one was frozen in liquid nitrogen for mRNA purification and further studies using real-time PCR on cDNA samples obtained by reverse transcription of mRNA samples (RT-Q-PCR). Most males were captured in December (n = 9) and July (n = 7) of 3 consecutive yr (2006–2008). According to the breeding cycle of *T. occidentalis* [25], these samples include sexually active and inactive males, respectively. In addition, some males were also captured in March (n = 9), when their testes were in the regression process.

Electron Microscopy Techniques

Small pieces of gonads (2 × 2 mm) were dissected out from fresh testes and fixed in Karnowski fixative (2.5% glutaraldehyde, 1% formaldehyde in 0.1 M cacodylate buffer) for 45–60 min. The pieces were then processed for dehydration and resin embedding following standard procedures, including postfixation in OsO_4. Semithin sections (0.8 μm thick) and ultrathin sections (50 nm thick) were cut with a Reichert Ultracut ultramicrotome. Semithin sections were mounted on glass slides and stained with toluidine blue. Ultrathin sections were stained with uranyl acetate and lead citrate and examined in a Zeiss 10C transmission electron microscope (TEM) at the Scientific Instrumentation Center of the University of Granada.

Immunostaining

Immunohistochemical staining for specific proteins was performed using the ABC Kit (Vector Laboratories), according to the manufacturer's instructions. The following primary antibodies and working dilutions were used in this study: claudin 11 (sc-25711; 1:200; Santa Cruz), connexin 43 (sc-9059; 1:100; Santa Cruz), N-cadherin (610920; 1:100; BD Biosciences), β-catenin (610154; 1:100; BD Biosciences), E-cadherin (610404; 1:100; BD Biosciences), SOX9 (sc-20095; 1:200; Santa Cruz), $P450_{scc}$ (sc-18043; 1:200; Santa Cruz), laminin (L-9393; 1:100; Sigma), α-smooth muscle actin (α-SMA) (A2547; 1:400; Sigma), proliferating cell nuclear antigen (PCNA) (sc-56; 1:100; Santa Cruz), and androgen receptor (AR) (sc-815; 1:100; Santa Cruz). Information on the full characterization of these antibodies is available in the respective product catalogs. For double immunofluorescence, AR + PCNA and claudin 11 + PCNA sections were incubated overnight with both primary antibodies, washed, incubated with the appropriate conjugated secondary antibodies 1 h at room temperature, and counterstained with 4′,6-diamidino-2-phenylindole (DAPI). Photographs were taken using an Olympus DP70 digital camera installed on an Olympus BX41 microscope. Three testicular sections of testes from breeding as well as nonbreeding males were consistently mounted on the same slide and processed together. Parallel negative controls were performed in which the primary antibody was omitted. Apoptotic cells were detected using the TUNEL technology, with an in situ cell-death detection kit (Roche).

Gene-Expression Quantification

Gene expression was quantified using real-time PCR on cDNA samples obtained by reverse transcription of mRNA samples (RT-Q-PCR). Freshly dissected mole testes were sliced into several sections and immediately immersed in liquid nitrogen, where they were stored until use. Total RNA was purified using an RNeasy kit (Qiagen), according to the manufacturer's procedures. DNAse I digestion was done to remove eventual contamination of the RNA samples with genomic DNA. The amount of RNA obtained was measured in a Nano-Drop 2000 instrument (Thermo Scientific) and the integrity of the RNA samples was tested by electrophoresis in 1% agarose gels. The lack of genomic DNA contamination in the RNA sample was assessed by performing a direct PCR amplification of a portion of the β-actin gene, a housekeeping gene known to be expressed in the mole testis. Reverse transcription was performed in 20-μl reactions, using 1 μg of total RNA with the Super-Script II kit (Invitrogen), according to the manufacturer's instructions (25°C for 5 min, 42°C for 30 min, 85°C for 5 min). Real-time PCR reactions were performed in a Chromo 4 thermal cycler (Bio-Rad), using the SensiMix SYBR kit (Quantace). The identities of all amplified fragments were confirmed by DNA sequencing. Amplification efficiency of 90%–105%, calculated from the slope of standard curves, was achieved for all the genes at their amplification temperatures. Gene-expression levels were calculated by the $-\Delta\Delta$CT method. *GAPDH* was used as a reference gene. The following primers were used: *CYP11A1* (cytochrome P450, family 11, subfamily A, polypeptide 1) F: AGG AGG GGT GGA CAC GAC; R: GTC TCC TTG ATG CTG GCT TT (fragment length = 177 bp, melting temperature [T_m] = 55°C); *AR* (androgen receptor) F: ATT TGG ATG GCT CCA GAT CA; R: GCT GAG CAG GAT GTG GAT TT (fragment length = 177 bp, T_m = 52°C); *CLDN11* (claudin 11; a Sertoli cell tight junction constitutive protein) F: TGA CTG TTC TTC CCT GCA TC; R: AGC CAA AGC TCA CGA TGG (fragment length = 169 bp, T_m = 50°C); GJA1 (gap junction protein alpha 1, also known as connexin 43; a gap junction constitutive protein) F: TGT GAT GCG AAA GGA AGA GA, R: GAT GAT GTA GGT TCG CAG CA (fragment length = 178 bp, T_m = 50°C); *GAPDH* (glyceraldehyde dehydrogenase; and a reference gene for quantification) F: GAT GAC ATC AAG AAG GTG, R: TCA TAC CAG GAA ATG AGC TTG (fragment length = 179 bp, T_m = 54°C). The testes of inactive male moles undergo severe shrinkage, so that the number of Sertoli cells per unit of testis weight or volume (numeric density) increases in the inactive testis by 2.5-fold with respect to the active one, as the number of Sertoli cells does not vary during testis regression [16]. Similarly, the numeric density of Leydig cells in inactive testes is 3.97-fold higher than in active ones. Therefore, we have corrected the expression values of *CLDN11* in the inactive testis by dividing them by 2.5, as this gene is expressed exclusively in Sertoli cells, and those of $P450_{scc}$ by dividing them by 3.97, as this gene is expressed in Leydig cells. A similar correction was not applied in the case of *AR* and *GJA1* because these genes are expressed in several cell types (see below).

BTB Permeability Experiments

To test the permeability of the mole BTB, we adapted the biotin tracer experiment described by Meng et al. [27] to this species. Sexually active and inactive male moles were anesthetized with 0.125% avertin (2,2,2-tribromo-

ethanol), their testes were exposed, and a total of 50 μl of 10 mg/ml EZ-Link Sulfo-NHS-LC-Biotin (Pierce Chemical Co.) was placed beneath the tunica albuginea, injecting at several points of the left testis. The tracer was freshly diluted in PBS containing 1 mM CaCl2. The right testis was also treated in a similar way, but only PBS with 1 mM CaCl2 was injected in this case as a control. The testes were placed again inside the body of the animals, which were killed 30 min after the tracer injections. The testes were immediately removed and fixed overnight in 4% paraformaldehyde. Treated and control testes were dehydrated, embedded in paraffin (Paraplast plus), and sectioned (7 μm thick) according to standard procedures. After deparaffination and rehydration, the tracer was detected by incubating the sections for 30 min with an Alexa Fluor 568-conjugated streptavidin solution (included in the tracer kit) at 25°C. For double detection of the tracer and claudin 11, immunofluorescence for claudin 11 was performed prior to the tracer-detection technique as described above. In any case, the sections were finally rinsed twice with PBS for 10 min, stained with DAPI, rinsed four additional times with PBS (20 min each), and mounted in Vectashield medium (Vector Labs).

Radioimmunoassay

Blood from which to obtain serum samples was collected from several male moles, stored at 4°C overnight, and centrifuged at 6000 rpm for 20 min at 4°C. The supernatant (serum) was stored at −80°C until used. Intratesticular fluid was prepared by homogenizing 500 mg of decapsulated mole testicular tissue in 100 μl of PBS. The homogenates were then centrifuged at 10 000 rpm for 20 min at 4°C, and the supernatant (testicular fluid) was stored at −80°C. Hormone concentrations in these samples were measured by radioimmunoassay (RIA) using the TESTO-CTK kit for testosterone (DiaSorin), according to standard procedures. Duplicate measurements were made for all animals in the same RIA. The analytical sensitivity of the kits was 0.02 ng/ml, the interassay coefficient of variation was ≤7.2%, and the intra-assay coefficient of variation was ≤8.1%.

RESULTS

Evidence for Live Germ-Cell Desquamation During Mole Testis Regression

The Iberian mole *T. occidentalis* undergoes seasonal variations in the size and morphology of its testes and epididymides over its reproductive cycle. In the animals analyzed in this study, testis weight was around 4-fold higher in the breeding season compared to the nonbreeding season, coinciding with previously reported data for this species [16, 25]. In testes with active spermatogenesis (active testes), large testicular tubules were present with a well-structured and organized seminiferous epithelium at the different stages of the spermatogenic cycle (Fig. 1A) and, accordingly, the epididymides were completely full of spermatozoa (Fig. 1B). Apoptotic cells and some cell debris were also visible but not abundant. Small clusters of Leydig cells occupied the reduced volume existing between seminiferous tubules in these testes (Fig. 1A). By contrast, testes of sexually inactive males (inactive testes) contained tubules with reduced size in comparison to those in the breeding season, and the seminiferous epithelium was thin and disorganized (Fig. 1C). As a consequence, the epididymides were completely devoid of spermatozoa in these transiently sterile males (Fig. 1D). In this case, Leydig cells formed a continuous cell matrix, and occupied most of the testicular volume (Fig. 1C). To investigate the cellular mechanism underlying testis regression, we studied the testes from males in this stage (March–April in southern Spain). The process appears to be quite rapid, as only 4 males captured in March were found to be just at the regression stage, the rest having already inactive or still active testes. In the testes of males undergoing testis regression, some seminiferous tubules showed the lumen to be filled with abundant round cells and cell debris (Fig. 1E). The same type of cells and cell debris, among which primary and secondary spermatocytes and spermatids could be recognized, appeared in the tubule of the epididymides adjacent to these testes (Fig. 1, F

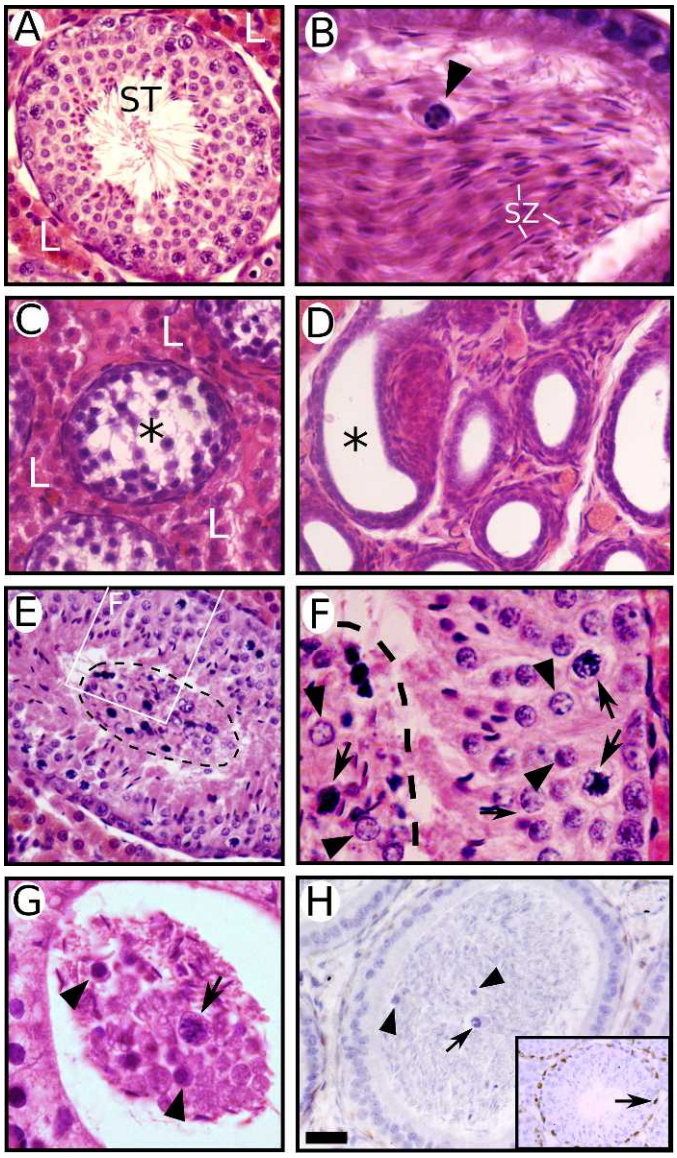

FIG. 1. Desquamation of the adluminal germinative epithelium at the end of the breeding season of the Iberian mole. **A**–**G**) Hematoxylin-eosin staining of testes (**A**, **C**, **E**, **F**) and epididymis (**B**, **D**, **G**) sections from moles captured during the breeding season (**A**, **B**), the nonbreeding season (**C**, **D**), and the testis-regression period (**E**, **F**, **G**). Active seminiferous tubules (ST in **A**) are large and contain a well-developed seminiferous epithelium, which is absent in the reduced tubules of inactive testes (asterisk in **C**). In contrast to that observed in active testes, Leydig cells (L in **A** and **C**) form a continuous cell matrix that occupies most testicular volume in inactive testes. The epididymis of active moles (**B**) is full of spermatozoa (SZ) with a few apoptotic cells (arrowhead), whereas it is completely empty (asterisk in **D**) in the nonbreeding season. During testis regression, some seminiferous tubules show the lumen filled with abundant round cells and cell debris (area outlined by a dashed line in **E**). **F**) Higher magnification of the area boxed in **E**, showing spermatocytes (arrows) and round spermatids (arrowheads) both in the germinative epithelium and in the lumen. **G**) The same cell debris could be observed in the epididymal tube (arrow, spermatocytes; arrowheads, round spermatids). **H**) Immunohistochemistry shows no SOX9-positive cell within the epididymis of a mole during the testis-regression period (arrows and arrowheads in **F**). Control SOX9-positive cells were found in the testis tubules of the adjacent testis (arrow in inset). Bar in **H** = 25 μm (**A**, **C**, **E**, **H**), 10 μm (**B**, **G**, **F**).

and G), where no recognizable spermatogonia were present. Furthermore, immunohistochemistry for SOX9, a Sertoli cell marker, revealed that Sertoli cells were not among the desquamated cells within the epididymal tubule (Fig. 1H).

Are Germ Cells Already Dead When Desquamated?

In an effort to determine whether the cells that desquamate from the germinative epithelium of regressing mole testes are either living or dead, histological sections of testes and epididymides from inactivating males were treated with the TUNEL technique, which detects both apoptotic and some necrotic cells. Very few apoptotic cells could be seen in each microscope field in these preparations and almost the totality of the desquamated cells (spermatocytes and spermatids at different maturation stages) were not stained either in the seminiferous (Fig. 2A) or in the epididymal (Fig. 2B) tubules, showing that they are alive at the moment when desquamation occurs.

Time Course of Mole Testis Regression

Although testis regression is a relatively fast event that does not affect all males simultaneously during the transition period between the breeding and the nonbreeding seasons, we identified two well-defined phases in this process, which, nevertheless, may occur simultaneously in different regions of the same testis (Fig. 3A). The first phase, which appeared to be longer, affected mainly the structure of the germinative epithelium and did not imply a substantial reduction in the diameter of the seminiferous tubules or thus in the whole testis weight and size (Fig. 3, B and C). The main event of this phase was the disorganization and slimming of the germinative epithelium, which showed deep projections of the tubular lumen towards the basal compartment, and the massive desquamation of the meiotic and postmeiotic cells of the adluminal compartment (Fig. 3, B, C, and F). These changes simultaneously affected most if not all seminiferous tubules, and this was the status in which the testes of most males can be observed in the transition period after the breeding season. In the second phase, once the seminiferous epithelium had lost most of the meiotic and postmeiotic cells, the diameter of the seminiferous tubules decreased rapidly until acquiring the size

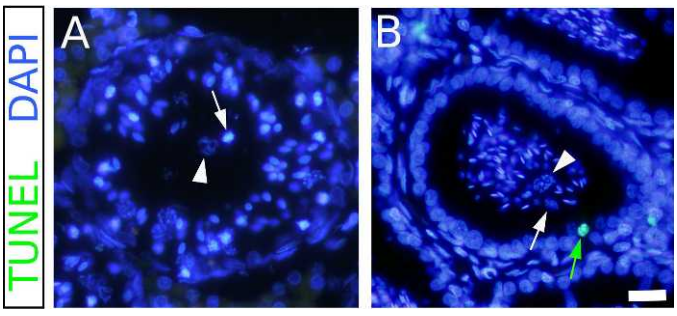

FIG. 2. Germ cells are still alive when they are desquamated. TUNEL analysis (green staining) followed by DAPI counterstaining (blue) of testis and epididymis of moles during the testis-regression period. Apoptotic cells were not detected among the desquamated cells observed in the lumen of either the testis tubules (**A**) or the epididymal tube (**B**). Arrowheads point to desquamated spermatocytes at zygotene-pachytene stage. Arrow in **A** points to a spermatocyte at the leptotene stage. White arrowhead in **B** points to a round-elongated spermatid. Green arrow in **B** points to a positive TUNEL-stained, apoptotic cell located at the epididymis epithelium. Apoptotic cells were very scarce both in the testes and in the epididymides. Individual color channels were adjusted for proper color visualization. Bar in **B** = 20 μm.

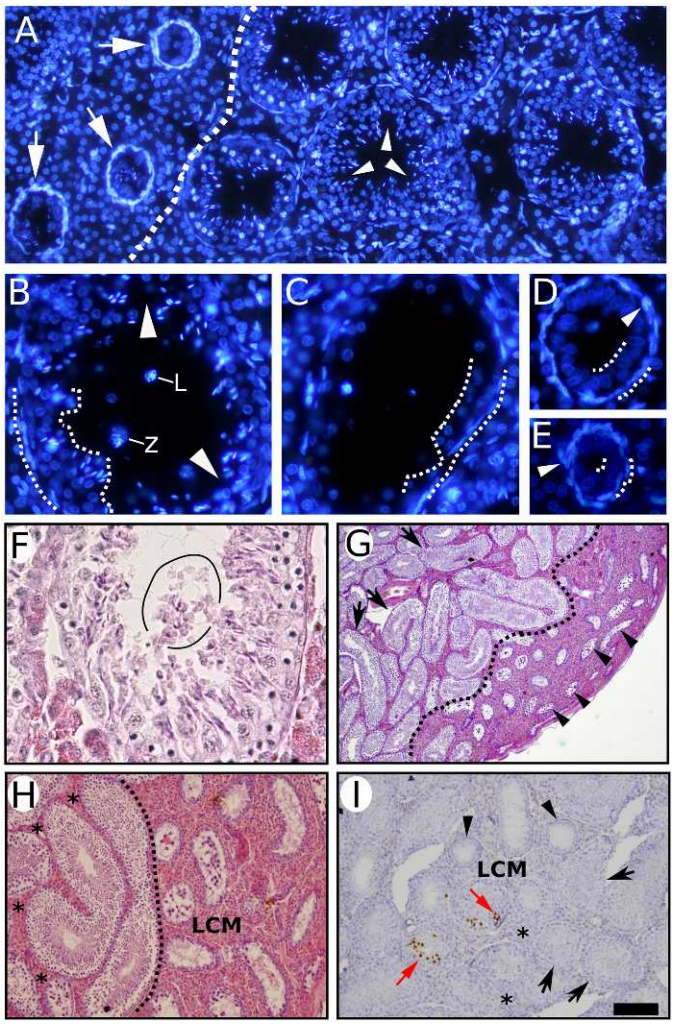

FIG. 3. Histology of the mole testes during the regression period. **A**–**E**) DAPI staining. At low magnification (**A**), some testes show a region with fully regressed testis tubules (arrows) and another region with not fully regressed tubules showing deep projections of the tubular lumen towards the basal compartment (arrowheads); the dashed line marks the separation between these two regions. Testis tubules at different stages of regression are shown in **B**–**E**. The number of cell layers decreases as the process proceeds, with four to five in **B**, two to three in **C**, and one to two in **D** and **E** (shown by space between the two dashed lines in **B**–**E**). In the most advanced stages of testis regression, peritubular myoid cells show a pseudostratified cell-layer aspect (marked with an arrowhead in **D**). **F**–**H**) Hematoxylin-eosin staining of mole testes sections in the regression stage. **F**) Desquamation of a group of cells (outlined) still maintaining contact with the germinative epithelium (line interruptions). **G**) Nonfully regressed testis tubules (arrows) on the left side of the dashed line, which are in the first phase of the testis-regression process, can be distinguished from those on the right, which are fully regressed testis tubules (arrowheads) in the second phase. **H**) Leydig cell clusters remain small and scattered (asterisks) among the seminiferous tubules in the first-phase tissue (left of the dashed line), but form a massive matrix that embeds the regressed tubules in the second-phase tissue (LCM, region to the right of the dashed line). **I**) Immunohistochemistry for PH3 shows that regressing testes contain some proliferating cells (red arrows) in the nonfully regressed testis tubules (arrows), but none in fully regressed ones (arrowheads) or in Leydig cells (asterisks). Bar in **I** = 30 μm (**B**–**E**), 60 μm (**A**), 120 μm (**G** and **H**), 300 μm (**F**).

observed in fully regressed testes (Fig. 3, D and E). As a consequence of the subsequent reduction in the external area of the tubules, the peritubular myoid cells, which covered them completely, formed deep overlapping infoldings showing the

aspect of an apparently multi-stratified cell layer. The completion of the second phase was regionalized and did not affect all the seminiferous tubules simultaneously. Testes in the second phase of regression contained two clearly delimited regions, one containing first-phase-type seminiferous tubules, and another one with seminiferous tubules showing the features of fully regressed testes. This region was generally observed in the vicinity of the rete testis and extended through the periphery of the testis, whereas the rest of the testis volume maintained the first-phase aspect (Fig. 3G). The relative size of the fully regressed testicular tissue varied between individual testes, depending on the degree of advance of the regression process. Apart from the diameter and contents of the seminiferous tubules, these two testicular regions differed greatly in the organization of the Leydig cell clusters. These were small and scattered among the seminiferous tubules in active testes as well as in those in the first phase of regression, but became a massive matrix of Leydig cells, where the regressed seminiferous tubules are embedded, in the second-phase regressing testes. This difference could be seen very clearly at the border region between the two types of testicular tissue (Fig. 3H). However, this process was not accompanied by a higher number of Leydig cells, as immunohistochemistry for phospho-HIST3H3 (PH3), a marker for proliferating cells, showed that Leydig cell proliferation remained at very low levels throughout the year and did not significantly rise during the testis-regression period (Fig. 3I). The second phase of mole testis regression was probably very fast, as only four animals out of the nine analyzed in the regression period were observed in this phase.

Ultrastructural Features of Active and Inactive Mole Testes

Sertoli-Sertoli specialized junctions, which constitute the BTB, showed clear differences between active and inactive mole testes. They were long, well-formed junctional complexes in the active testes (Fig. 4A), but were almost completely absent in those of inactive moles. The intermediate situation was observed in testes of the two transition periods (Fig. 4B). In active testes, Sertoli cells showed a relatively low numeric density (estimated in this case as the number of cells per section area unit), most of the germinative epithelium volume being occupied by spermatogonia and meiotic and postmeiotic cells, including spermatocytes and spermatids of different types (Fig. 4C). The cytoplasm of Sertoli cells in these testes was quite electron dense and contained numerous organelles. The cell membranes and the space between adjacent Sertoli cells appeared normal. This type of Sertoli cell persisted in the regressing testes, but coexisted with Sertoli cells exhibiting a very light cytoplasm containing a lower number of organelles (Fig. 4D). These pale Sertoli cells constituted the only somatic cell type found in in the seminiferous tubules of fully regressed, nonspermatogenic, inactive testes. These cells filled most of the volume occupied by the narrow germinative epithelium of these testes, as they contained very few meiotic and postmeiotic cells (Fig. 4E). Their cytoplasm was extremely reduced and the numeric cell density was thus very high in these inactive testicular tubules. This reduction of the cytoplasmic volume of Sertoli cells was not accompanied by a parallel reduction in the size of their cell membranes, which appeared to remain stored in the form of repeated and superposed membrane infoldings (Fig. 4, F and G). In addition, the cell membranes of adjacent Sertoli cells appeared to become fused to each other in regular spots and were more electron dense that those of Sertoli cells in active testes (Fig. 4H). The cytoplasm of Leydig cells in active testes (Fig. 4I) was more dense and contained more mitochondria than that of inactive ones (Fig. 4J). Seasonal differences were also observed in the intercellular spaces between Leydig cells, which showed a less profuse system of cell interdigitations and a less electron-dense matrix in active (Fig. 4K) than in inactive testes (Fig. 4L). Further quantitative analyses are required to confirm these observations.

Analysis of the BTB Functionality

The lack of normal BTB structures observed by electron microscopy in the testes of inactive male moles suggested that BTB functionality could be compromised in these animals. To test whether the BTB of nonbreeding mole testes becomes permeable to small molecules (<600 Da), we injected a biotin tracer into the interstitial space of both active and inactive mole testes. In active testes, the biotin tracer was located in the interstitial region and in the basal compartment of testis tubules, but no positive signal was found in the adluminal compartment (Fig. 5A). By contrast, the biotin tracer was found in the interstitial region and throughout the entire germinative epithelium of the inactive testis tubules, reflecting impaired BTB impermeability (Fig. 5B). The lack of BTB functionality can also be evidenced by identifying the cell types observed in the seminiferous tubules of inactive moles. We have recently reported that cells showing a robust expression of PCNA (a cell marker specific for spermatogonia and early primary spermatocytes) were found exclusively in the basal compartment of the active testes [28]. To check whether these cell types can move to the adluminal compartment in inactive testes, we performed double immunofluorescence for claudin 11 (a BTB marker; see below) and PCNA. In active testes, PCNA-positive germ cells were located exclusively in the basal compartment, whereas the adluminal compartment contained only PCNA-negative cells, corresponding to germ cells in a more advanced stage of spermatogenesis (Fig. 5C). Contrarily, almost all the cells in the adluminal compartment in tubules of inactive testes were clearly PCNA positive (Fig. 5D), indicating that no barrier was operating in this case, despite that claudin 11 protein was present also in these regressed tubules.

Expression and Distribution of Cell-Adhesion Molecules in Active and Inactive Mole Testes

Our transmission electron microscopy study of inactive mole testes revealed alterations in the Sertoli-Sertoli and Sertoli-germ cell junctional structures. To assess whether the expression of proteins composing these cellular junctions were altered, we performed immunohistochemistry for a number of cell-adhesion proteins. Claudin 11 is a member of the tight junction transmembrane protein superfamily expressed in brain, testis, choroid plexus, and kidney [29]. In the testis, this protein is expressed in tight junctions located between Sertoli cells at the site of the BTB (reviewed in [30]). In the mole, immunohistochemical analysis revealed a dynamic spermatogenic cycle-dependent pattern of claudin 11 expression in active testes (Fig. 6A). To determine the stages of the spermatogenic cycle of *T. occidentalis*, we followed the criteria reported previously by Sánchez et al. for this species [31]. In active testes (Fig. 6A, a–e), stages I–III showed claudin 11 immunoreactivity very close and parallel to the basal surface of the testis tubules, forming a belt with numerous discontinuities (Fig. 6Aa). In stages IV–VI the latter pattern of expression was maintained, but a more continuous and stronger belt of protein staining, located slightly more separately from the basal

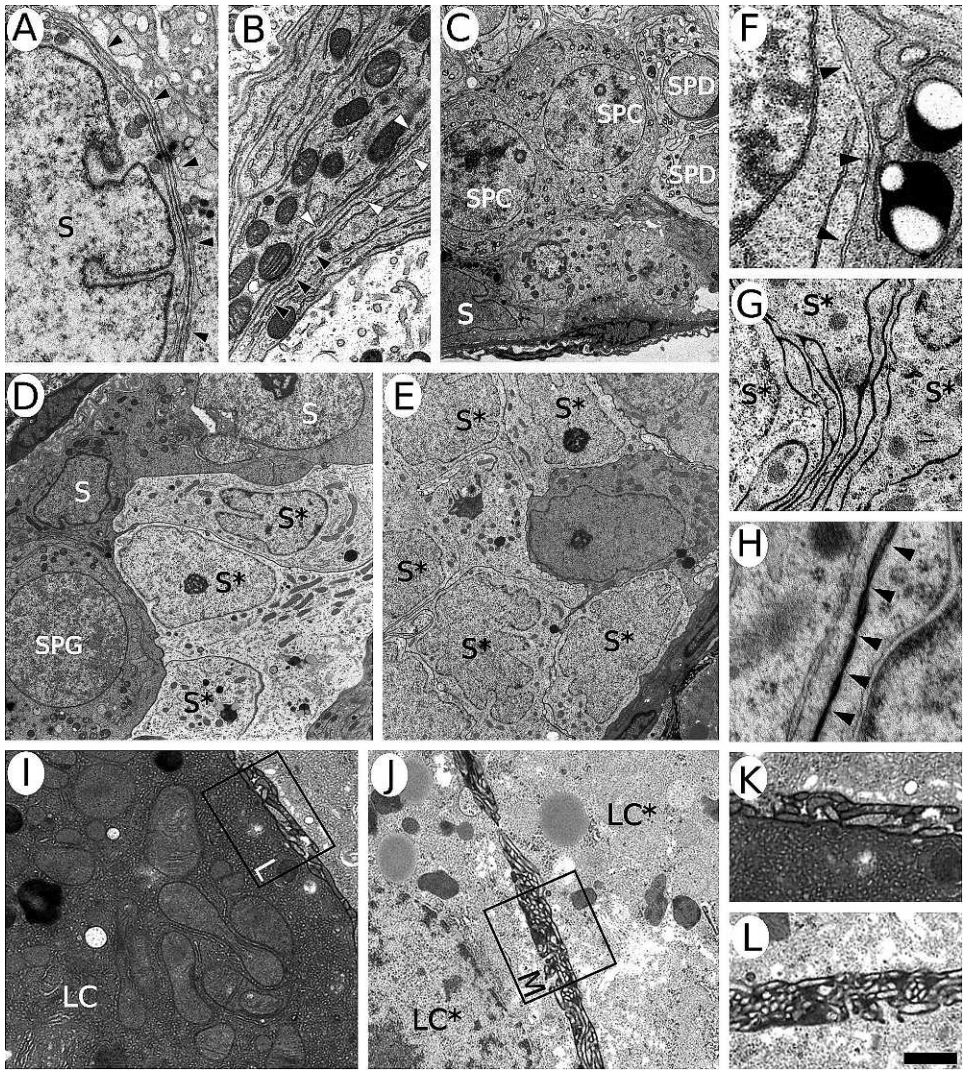

FIG. 4. TEM ultrastructural analysis of functional and regressed mole testes. **A** and **B**) Analysis of the BTB. **A**) In active testes, BTB junctional complexes (black arrowheads) between Sertoli cells (S) are long and well formed. **B**) In regressing testes, BTB complexes show frequent discontinuities (white arrowheads). **C**) Active testes contain electron-dense Sertoli cells (S) with low numeric density; most of the space is occupied by germ cells (SPC, spermatocytes; SPD, round spermatids). **D**) In regressing testes, the type of Sertoli cell (S) described in **C** coexists with another type exhibiting a paler cytoplasm (S*) (SPG, spermatogonia). **E**) In fully regressed testes, all Sertoli cells show a pale cytoplasm (S*) and occupy most of the space of the narrow germinative epithelium. **F**–**H**) Alterations of the cell membrane in Sertoli cells. **F**) In the active testis, cell membranes from adjacent Sertoli cells appear as a continuous, unfolded, thin double line (arrowheads). **G**) By contrast, in the inactive testis, membranes of pale Sertoli cells (S*) show repeated and superposed infoldings and a dense intercellular matrix. **H**) At a higher magnification, these membranes appear to become fused to each other in regular spots (arrowheads) and are more electron dense than those of Sertoli cells in active testes. **I**) The cytoplasm of Leydig cells (LC) in active testes is dense and contains abundant mitochondria. **J**) That of Leydig cells in the inactive testes (LC*) is less dense and contains fewer organelles. **K** and **L**) Higher magnification of the areas boxed in **I** and **J** showing that the intercellular spaces between Leydig cells indicates a less profuse system of cell interdigitations and contains a less electron-dense matrix in active (**K**) than in inactive (**L**) testes. Bar in **L** = 0.25 μm (**H**), 0.50 μm (**F**, **G**, **K**, and **L**), 0.90 μm (**I** and **J**), 1 μm (**A** and **B**), 3 μm (**C**–**E**).

lamina, was now observed (Fig. 6Ab). In stages VII–VIII, an almost continuous and strongly stained belt of protein was present, separated from the basal surface by a monolayer of cells (Fig. 6Ac). This expression pattern changed in stage IX, where claudin 11 staining appeared at the vicinity of the basal lamina, with no continuity or particular orientation and involving several cell layers (Fig. 6Ad). In stage X, the same pattern persisted but the staining intensity became much weaker (Fig. 6Ae). Inactive testes also showed a dynamic claudin 11 expression pattern, but protein distribution was more diffuse and irregular (Fig. 6A, f–h). Although normal germinative epithelium dynamics are eliminated in inactive mole testes, claudin 11 staining helped us to establish a staging resembling that of active testes. In the I–IV-like stage, a diffuse protein belt was separated from the basal lamina of the seminiferous tubule by a monolayer of cells, thus defining apparent adluminal and basal compartments (Fig. 6Af). In the VII-like stage, a more strongly stained belt of claudin 11 separated these two compartments, and in some seminiferous tubules, the basal one was formed by a multilayer of cells (Fig. 6Ag). In the VIII–I-like stage, claudin 11 immunostaining appeared more disorganized within the multilayer of cells that composed the germinative-like epithelium of the inactive testis tubules (Fig. 6Ah). Quantification of claudin 11 gene (*CLDN11*) expression levels by RT-Q-PCR revealed a 11.5-fold reduction in inactive testes with respect to active ones (Fig. 6Ca).

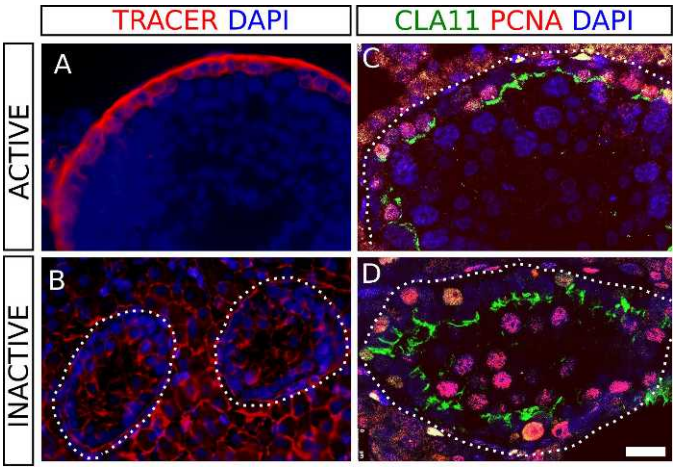

FIG. 5. The BTB is permeated in inactive mole testes. **A**, **B**) Test of BTB functionality using a biotin tracer (red fluorescence) and DAPI counterstaining (blue fluorescence). In the active testis (**A**), the tracer did not penetrate beyond the basal compartment, whereas in the inactive testis (**B**) it reached the deepest areas of the regressed seminiferous tubules (outlined by dashed lines). **C**, **D**) Double immunofluorescence for PCNA (red), a marker for spermatogonia and early primary spermatocytes, and for claudin 11 (green), a tight junction protein involved in BTB structure, followed by DAPI counterstaining. In active testes (**C**), PCNA-positive germ cells are located exclusively in the basal compartment, whereas almost all the cells in the adluminal compartment of regressed tubules in inactive testes (outlined by dashed lines) are PCNA positive (**D**). Individual color channels were adjusted for proper color visualization. Bar in **D** = 10 μm (**C** and **D**), 20 μm (**A** and **B**).

We next analyzed the expression pattern of connexin 43 (indicated as CNX43 in Fig. 6B, a and g), a component of the gap junctions found in the interstitial Leydig cells as well as in Sertoli-Sertoli and Sertoli-germ cell contact areas, which is expressed in a spermatogenic cycle-dependent manner located mainly in the basal compartment of seminiferous epithelium [32]. Whereas in active-testis expression, spots were clearly more abundant in the adluminal compartment (Fig. 6Ba), in inactive testes connexin 43 staining was detected throughout the regressed germinative epithelium (Fig. 6Bg). In addition, connexin 43 immunoreactivity in Leydig cells was stronger in inactive than in active testes. Quantification of connexin 43 gene (*GJA1*) expression levels by RT-Q-PCR showed a 2.0-fold reduction in inactive testes with respect to active ones (Fig. 6Cb). Also, we analyzed the expression pattern of three additional molecules, β-catenin and E- and N-cadherin (Fig. 6B, b–d and h–j), which are structural components of the adherens junctions as well as of the ES located adjacent to the Sertoli-Sertoli and Sertoli-germ cell contact areas [33]. In active testes, immunoreactivity for the three molecules was relatively stronger in the basal than in the adluminal region, which showed a faint staining (Fig. 6B, b–d). By contrast, inactive testes showed a homogeneous staining for the three molecules throughout germinative-like epithelium depth (Fig. 6B, h–j). In addition, we checked whether the integrity of the lamina propria, the structure that envelops the seminiferous tubules and separates the seminiferous epithelium from the interstitium of the male gonad, was impaired throughout the breeding cycle of the mole (Fig. 6B, e, f, and k–l). Immunohistochemistry for laminin, a major component of the basement membrane, and for α-SMA, a marker for peritubular myoid cells, showed no difference in the expression pattern of the two molecules, indicating that the lamina propria maintains its integrity throughout the breeding cycle of the mole.

Androgenic Function in Active and Inactive Mole Testes

Variations in the levels of testicular hormones are associated with changes in testicular features, including the expression of cell-adhesion molecules, integrity of the BTB (see [34]), spermatogenesis, and testicular size (reviewed in [35]). All these features are altered in nonbreeding mole testes. We have previously demonstrated that serum testosterone levels vary throughout the breeding cycle of *T. occidentalis* [18], but, in the light of our new findings, we extended our study to other molecules involved in androgenic function. Using RIA, we measured the serum and intratesticular levels of testosterone. Consistent with our previously published data, inactive moles showed a 4.7-fold reduction of serum testosterone levels when compared to active moles (Fig. 7Aa). Similarly, the measurement of intratesticular testosterone levels showed a 5-fold reduction in inactive testes when compared to active testes (Fig. 7Ab). Next, we studied the expression pattern of AR, the cellular mediator of the physiological effects of androgens. Immunohistochemistry revealed that AR is expressed in cells located in the basal region within seminiferous tubules, in peritubular myoid cells, and in the interstitial Leydig cells (Fig. 7Ba). Because it is controversial whether the AR within the testis cords is expressed in germ cells in addition to Sertoli cells (see [36]), we performed double immunofluorescence for AR and PCNA, which marks spermatogonia and primary spermatocytes (see above). We observed either AR- or PCNA-positive cells, but never coexpression of both proteins, showing that AR is expressed exclusively by Sertoli cells within the mole testis tubules (Fig. 7Bb). In inactive testes, the AR expression pattern was similar to that shown in active testes, although the intensity of the immunostaining was weaker (Fig. 7Bc). This latter observation was confirmed by RT-Q-PCR, which revealed a significant 2-fold reduction in the level of AR transcripts with respect to those in active testes (Fig. 7Bd). Finally, we studied the expression of the cytochrome $P450_{scc}$ (side-chain cleave), an enzyme involved in testosterone production. Using immunohistochemistry, we detected $P450_{scc}$ expression in the interstitial Leydig cells of active as well as inactive testes, although the staining again appeared to be weaker in the inactive period (Fig. 7C, a and b). Consistently, RT-Q-PCR for $P450_{scc}$ showed a 4.7-fold reduction in the expression levels of this gene in inactive testes, confirming the immunohistochemical observations (Fig. 7Cc).

DISCUSSION

Live Germ-Cell Desquamation: A New Mechanism for Seasonal Testis Regression

In seasonal breeders, the transition from the breeding to the nonbreeding periods involves a process of testis regression that is not well understood in mammals or other vertebrates. Here, we report on a detailed study of several aspects of the changes occurring in the testes during the circannual reproductive cycle of the Iberian mole, *T. occidentalis*, and found that the regression of the testicular tissue in the mole is a fast process that takes place in two phases. In the first, the adluminal compartment of the germinative epithelium is lost, and in the second, the seminiferous tubules decrease in diameter and are embedded in a dense matrix of Leydig cells. This second phase involves major cell and tissue remodeling, starting in the vicinity of the rete testis and proceeding according to a centripetal wave. The mechanism of testis regression described here for the Iberian mole has not been reported before in any other seasonal breeding mammal.

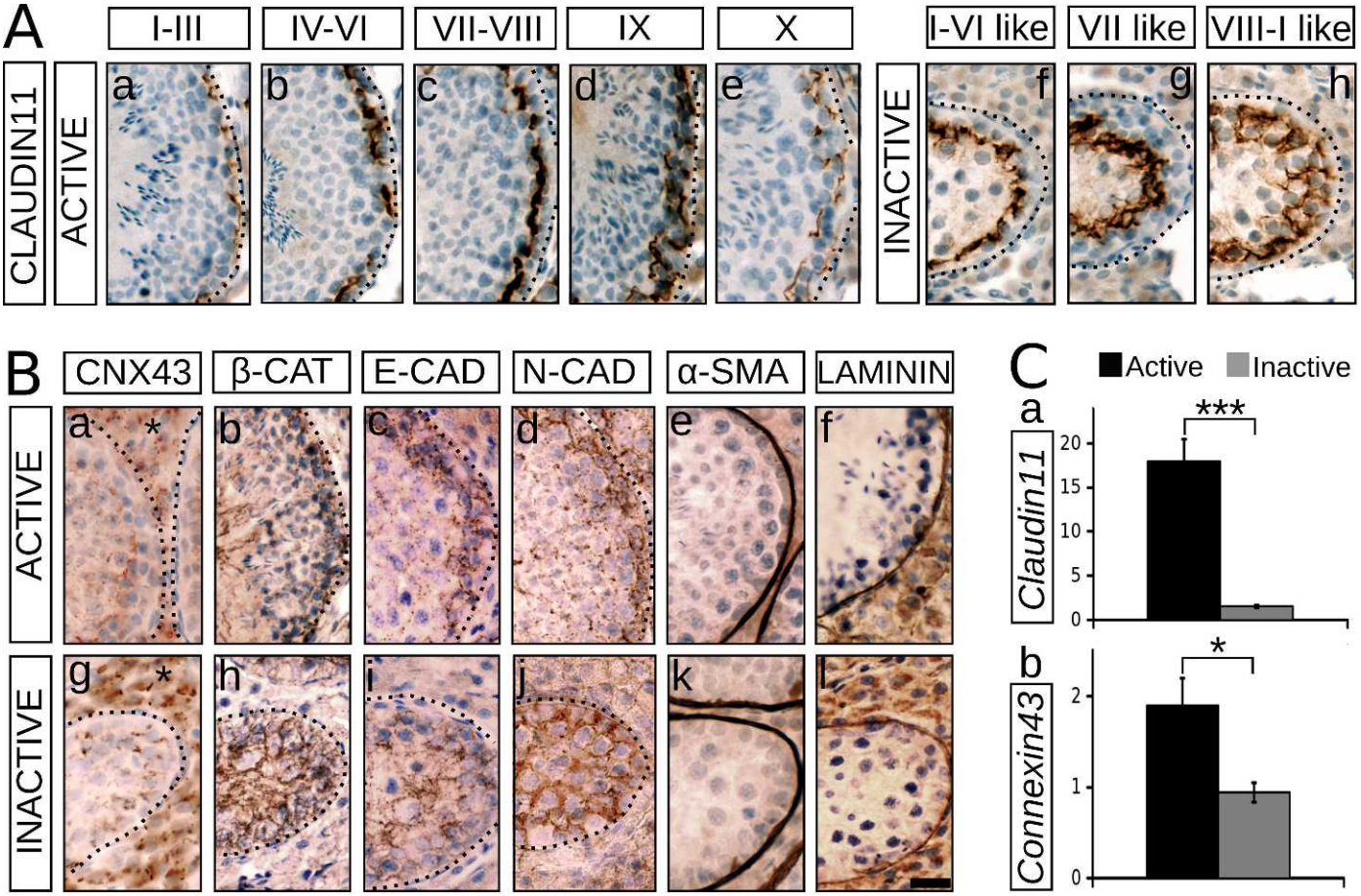

FIG. 6. Expression of cell-adhesion molecules in active and inactive testes. **A**) Immunohistochemistry for claudin 11 in active (**a**–**e**) and inactive (**f**–**h**) mole testis sections. In active testes, claudin 11 shows a dynamic pattern of expression throughout the spermatogenic cycle (stages I–X; **a**–**e**). In inactive testes, this pattern of expression is altered. Some spermatogenic-like stages resembling those defined for active testes are shown (from I–VI to VIII–I; **f**–**h**). **B**) Immunohistochemistry for connexin 43 (CNX43; **a**, **g**), β-catenin, (β-CAT; **b**, **h**), E-cadherin (E-CAD; **c**, **i**), N-cadherin (N-CAD; **d**, **j**), α-SMA (**e**, **k**) and laminin (**f**, **i**) in active (**a**–**f**) and inactive (**g**–**l**) mole testis sections. Note that the pattern of expression for connexin 43, β-catenin, E-cadherin, and N-cadherin in inactive testes is altered in comparison to that of active testes (asterisks in **Ba** and **Bg** mark the areas occupied by Leydig cells). By contrast, the expression patterns of α-SMA and laminin remain unchanged in active and inactive testes. **C**) Quantification of the transcripts levels of claudin 11 (**a**) and connexin 43 (**b**). Bar in **Bl** = 20 μm (all).

Whereas germ-cell apoptosis has been postulated as the major (or the only) testis-regression effector in most species with seasonal breeding (discussed below), the present study clearly shows that, in the mole, germ cells are eliminated from the germinative epithelium by a process of desquamation without any previous significant contribution of apoptosis, implying that most germ cells discarded during testis regression in this species are alive at the moment of being expelled from the testis and entering the epididymal tube. Although massive depletion of germ cells has been described in other species and is considered generally a consequence of previous germ-cell death by apoptosis (reviewed in [35, 37]), this is the first instance in which desquamation of living germ cells is identified as a major mechanism for seasonal testis regression. Previously, we reported that the numeric density of apoptotic germ cells is very low during mole testis regression, being higher during the nonbreeding season. This pattern is consistent with a role for apoptosis in the elimination of the primary spermatocytes that continue to be produced in the inactive period, as a consequence of the fact that mole spermatogonia do not stop entering meiosis [16].

Seasonal Sertoli and Leydig Cell Remodeling

The depletion of most of the adluminal portion of the germinative epithelium during mole testis regression implies a dramatic remodeling of the somatic cells of the gonad. The great reduction in the seminiferous-tubule diameter forces Leydig cells to accommodate to the new available intertubular space, forming a continuous matrix of interstitial tissue in which the much thinner tubules are finally embedded. This process occurs during the second phase of testis regression and, in the mole, is much more conspicuous than in other mammalian species. Because we detected no significant variation in the levels of apoptosis and cell proliferation in mole Leydig cells over the seasonal breeding cycle, as reported for the roe deer [38], this remodeling is probably mediated by active cell movement.

The cytologic transformation that Sertoli cells undergo during testis regression is even more severe. We have previously reported that the number of Sertoli cells remains invariable throughout the breeding cycle, suggesting that these cells are either not affected by apoptosis or affected to a similar magnitude at all the stages of the cycle [16]. Here we report that the numeric density of Sertoli cells was higher in inactive than in active testes, showing that these cells reduce their

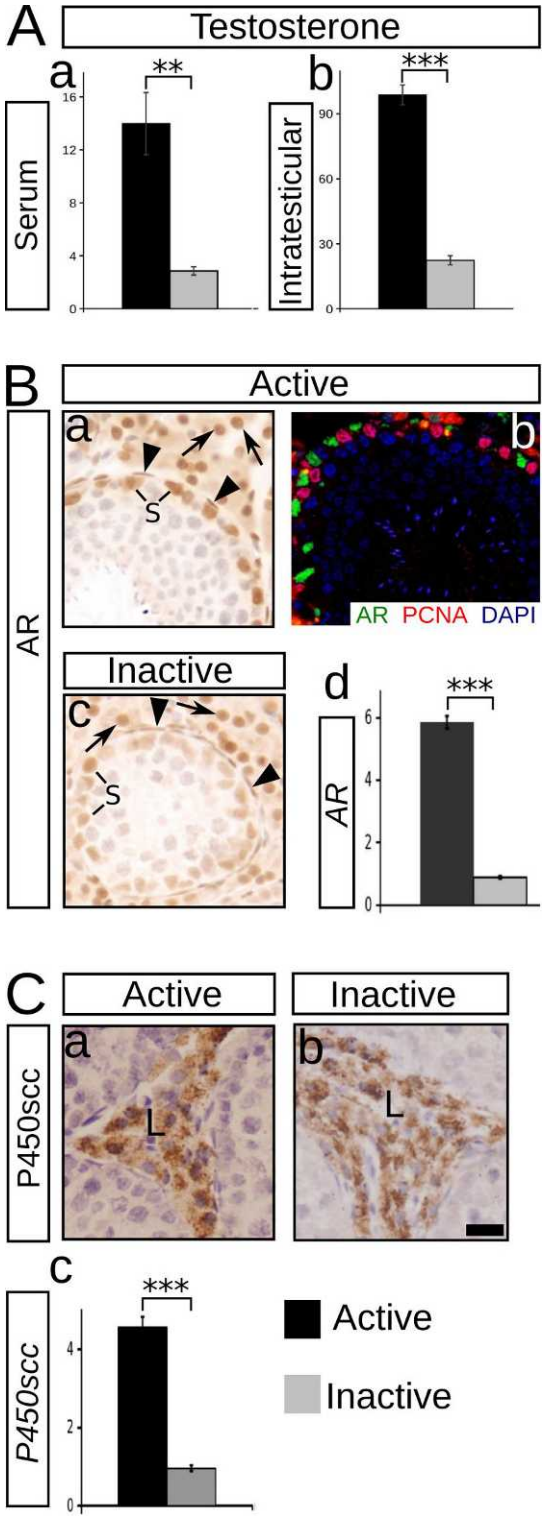

FIG. 7. Androgenic function of active and inactive mole testes. **A**) RIA analysis of serum (**a**) and intratesticular (**b**) testosterone levels in active and inactive moles. Inactive moles show a 4.7-fold reduction of serum testosterone levels in comparison to that of active testes (13.98 ± 2.34 ng/ml and 2.85 ± 032 ng/ml; unpaired Student *t*-test, $^{**}P = 0.0033$). Likewise, the levels of intratesticular testosterone show a 5-fold reduction in inactive moles in comparison to those of active moles (98.73 ± 4.58 ng/g and 24.38 ± 2.12 ng/g; unpaired Student *t*-test, $^{***}P < 0.0001$). **B**) Expression pattern of AR. **a**) Immunohistochemistry in active mole testes showing AR expression in Sertoli cells (S), peritubular myoid cells (arrowheads), and Leydig cells (arrows). **b**) Double immunofluorescence for PCNA (red), a marker of germ cells, and for AR (green) followed by DAPI counterstaining (blue) revealed no coexpression of either protein, indicating that AR is exclusively expressed by Sertoli cells within active seminiferous tubules. **c**) Immunohistochemistry in inactive mole testis sections shows that AR is expressed in the same cell types as in active testes, although the staining looks weaker. **d**) RT-Q-PCR showed a 6-fold reduction in the transcript levels of *AR* in the inactive testes in comparison to that of active testes (5.85 ± 0.2 and 0.9 ± 0.03; unpaired Student *t*-test, $^{***}P < 0.0001$). **C**) Expression of cytochrome $P450_{scc}$ (side-chain cleavage). **a**, **b**) Immunohistochemistry revealed expression for $P450_{scc}$ in Leydig cells (L) in both active and inactive mole testis, although in the inactive testis the staining looks slightly weaker. **c**) The RT-Q-PCR showed a 4-fold reduction in the transcripts levels of $P450_{scc}$ in inactive testes in comparison to that of active ones (4.55 ± 0.27 and 0.96 ± 0.07; unpaired Student *t*-test, $^{***}P < 0.0001$). Bar in **Cb** = 10 μm (**Ca**, **Cb**), 20 μm (**Ba**–**Bc**).

volume considerably during testis regression. This is consistent with our finding [16] that the number of Sertoli cells per seminiferous-tubule cross section is not significantly higher in inactive testes, even when the same number of these cells is enclosed in a smaller volume because of testis shrinkage. A detailed ultrastructural and morphometric study of viscacha (*Lagostomus maximus maximus*) Sertoli cells during the annual reproductive cycle [39] described several pieces of cytological evidence supporting the functional involution in the regressed testis (also observed in the mole; see below), but the authors reported no variation in the cell volume, which agrees with their finding that the number of Sertoli cells per tubular cross section decreased significantly during testicular regression. Moreover, no variation was detected in the viscacha Sertoli cell membrane, other than those related to cell junctions. In the mole, however, Sertoli cells appear to retain most, if not all, of the cell membrane during the drastic volume reduction in the testis regression stage. This induces the formation of large regions occupied by superposed membrane infoldings, a phenomenon that has not previously been reported. We presume that the same cell membranes are reused during the subsequent testis recovery and that this represents a clear example of cell economy.

Most of the cytological features observed in Sertoli cells in regressed testes provide evidence that these cells undergo a severe functional involution during testis regression: 1) the reduction of cell volume, 2) the lower number of cell organelles, 3) the paler cytoplasm, 4) the permeation of the BTB, and 5) and the disassembly of the apical ES. The systematic death by apoptosis of the primary spermatocytes that continue to be produced in the inactive mole testis [16] is probably a consequence of the lack of supporting functional Sertoli cells in these gonads.

Reduction and Remodeling of Cell-Adhesion Molecules Explain Germ-Cell Desquamation

The most reasonable explanation for massive germ-cell depletion by desquamation of the germinative epithelium is that the cell junctions maintaining the architecture of this tissue become disorganized. The most prominent structure derived from Sertoli-Sertoli cell junctions is the BTB, which contains multiple types of cell junctions [8, 33, 40–44], and additional junctions are also established between Sertoli cells and germ cells (see [43–45]. In the mole, the occurrence of germ-cell desquamation indicates that most, if not all, of these structures must be impaired to permit germ cells to detach from Sertoli cells. This implies that major changes in the composition and organization of the cell-adhesion molecules making up these cell junctions must occur during this process. In this sense, we have found several pieces of direct and indirect evidence: 1) the

BTB functionality is compromised during testis regression, becoming permeable in inactive testes; 2) quantification by RT-Q-PCR of the expression of *CLDN11* and *GJA1* (two genes encoding principal components of tight junctions and adherens junctions, respectively) showed a significant lowering of the messenger levels of these two genes in the nonbreeding period; 3) immunohistochemical studies of the expression pattern of these two proteins as well as β-catenin, N-cadherin, and E-cadherin, which are components of the multi-protein complexes forming ES (reviewed by Kopera et al. [44]), showed clear alterations in the inactive testes with respect to the active period; and 4) electron microscope analysis showed that the intermembrane space separating adjacent Sertoli cells in nonbreeding testes was irregular in shape and filled by a dense intercellular matrix.

Hence, in the mole, the circannual variations in the cell-content dynamics of the seminiferous epithelium is regulated by modulating the expression and functionality of the cell-adhesion molecules comprising the different types of testis-specific cell junctions, a process by which a massive germ-cell depletion takes place once every year and marks the end of each breeding season. Such a mechanism of seasonal breeding regulation had not been described previously in any other vertebrate species.

Germ-Cell Desquamation and BTB Permeation Must Occur Sequentially and Be Regulated Separately

One of the most relevant functions of the BTB is to sequester postmeiotic germ cells from the systemic circulation, thereby avoiding the production of antibodies against the animal's own sperm [5, 33, 46]. Even when preleptotene spermatocytes pass from the basal to the adluminal compartment, traversing the BTB, this remains impermeable (reviewed in [43]). Here, we have shown that the BTB of male moles remains disorganized and permeable throughout the period of seasonal spermatogenic inactivity, a situation that might eventually lead to a process of auto-immuno-sensitization against postmeiotic germ cells, resulting in irreversible (nonseasonal) infertility. However, this is not the case, as these males become fertile again with each new breeding season, demonstrating that their immunological system had in fact no chance to make contact with these cell types. A plausible explanation is that no postmeiotic germ cell is present in the mole testis when the BTB permeation occurs, implying that germ-cell desquamation occurs before BTB permeation. In this way, postmeiotic germ cells would have disappeared from the adluminal compartment of the seminiferous epithelium by the time that the BTB is opened. Although we could not test the BTB functionality in male moles at the precise moment when germ-cell desquamation occurs (this being quite a fast process), two of our observations support this hypothesis: 1) during testis regression the first event to occur is indeed the desquamation of meiotic and postmeiotic germ cells (the first phase described above); 2) only germ cells from the adluminal compartment are depleted, suggesting that those of the basal compartment retain their junctional organization intact, including the BTB structure. Hence, BTB disassembly probably occurs once germ-cell desquamation is complete, implying that the regulatory mechanisms controlling the assembly and disassembly of Sertoli-Sertoli cell junctions (BTB) must be independent of those controlling adluminal Sertoli-germ cell junctions and should act separately to permit germ-cell desquamation without compromising BTB functionality. Once the BTB is permeated, the elimination by apoptosis of the primary spermatocytes produced during the nonbreeding period [16] would guarantee that no postmeiotic germ cell would be detected by the immunological system at this stage.

Testis Regression in the Mole Is Mediated by Intratesticular Androgen Suppression

There is compelling evidence that testicular cell-junction dynamics is regulated by hormones, but the intimate mechanisms of this process remain unclear. In the Djungarian hamster, photo-inhibited animals lose BTB functionality, indicating that follicle-stimulating hormone (FSH) has a key role in the regulation of Sertoli-Sertoli tight junctions [47]. In line with this, McCabe et al. [48] have recently shown that gonadotropins regulate rat testicular tight junctions in vivo. On the other hand, Sertoli cell-specific ablation of *AR* indicates that: 1) testosterone regulates BTB permeability by controlling the expression of *CLDNN3* (claudin 3), a transient component of newly formed tight junctions [27]; and 2) this BTB permeation leads to the loss of testicular immuno-privilege [49]. Moreover, Gye [50] and Florin et al. [51] have shown that androgens upregulate claudin 11 expression in primary cultures of mouse and rat Sertoli cells in vitro, whereas Kaitu'u-Lino et al. [52] have reported that both FSH and testosterone regulate the expression and localization of claudin 11 and the subsequent formation of tight junctions between rat Sertoli cells cultured in vitro. Notably, the situation in the mole reproduces, in a natural way, the experimental results reported by Xia et al. [53] in the rat. These authors found that intratesticular androgen suppression, induced by the administration of testosterone implants, led to a massive germ-cell depletion affecting only the adluminal compartment of the rat seminiferous tubule and showing that the disruption of adherens junctions was limited to the Sertoli-germ cell interface without perturbing the BTB. In the present study, we show that the androgenic function of male moles is highly diminished during the nonbreeding season, with a decrease of around 80% in the intratesticular levels of testosterone. Thus, as in the rat, this appears to be the hormonal signal inducing seasonal germ-cell depletion in the mole.

Hence, according to current data, the question as to whether BTB permeability is controlled by FSH or testosterone or both hormones remains controversial. Studies in rats [53] and Djungarian hamsters [47] appear to contradict those reported by other authors, as only the former studies suggest no role for testosterone in the control of the BTB permeability. Nevertheless, this controversy could be only apparent because equivalent experimental situations were not assessed in all cases. Whereas a complete ablation of the androgenic function was induced in the Sertoli cells of AR mutant mice [27, 49], or medium without testosterone was used in rat Sertoli cell cultures [52], the levels of intratesticular testosterone were considerably reduced, but probably not completely eliminated, either in the rats subjected to experimental androgen suppression [53] or in moles during the germ-cell desquamation phase. It is possible that Sertoli-germ cell adherens junctions (apical ES) and Sertoli-Sertoli tight junctions (BTB) require different concentrations of testosterone to be maintained. Thus, a reduction of the intratesticular hormone levels beyond a given threshold would lead to the disassembly of the apical ES and thus to a massive germ-cell desquamation, whereas a further reduction to an even lower threshold would be necessary to induce BTB permeation. FSH could either modulate the effects of testosterone on the BTB or regulate it independently.

Contrary to the suggestion that hormonal strategies for male contraception may interfere with the BTB [27], our results

show that the possibility exists that a transient postmeiotic germ-cell depletion (and hence transient infertility), mediated by intratesticular androgen suppression, can be produced without perturbing the BTB functionality, a process that moles appear to undergo naturally. This represents a promising development in the field of male contraceptive research.

Apoptosis Versus Desquamation as Testis-Regression Effectors

Many studies have been reported in the last two decades regarding the causes of seasonal testis regression in a number of vertebrate species, including reptiles, amphibians, birds, and mammals. A new paradigm emerges from these studies: that apoptosis is the main, if not the only, cell process mediating seasonal testis involution in most species (reviewed in [35, 37]). However, the existence of exceptional species in which apoptosis is clearly not the cause of testis regression, the roe deer [15] and the Iberian mole [16] (present study), requires a reconsideration of the paradigm. A detailed examination of the literature led us to classify the vertebrate species studied into three main groups. The first includes species in which the involvement of apoptosis in testis regression can be considered to be clearly established for two reasons: 1) the frequency of apoptotic cells increases and reaches a peak only during the period of testis regression and not later, when testis regression has finished and the testis shows a complete spermatogenic inactivity; 2) the magnitude of the apoptosis increase is high enough to explain a massive depletion of the germinative epithelium. The following species could be included in this group: the Japanese red-bellied newt *Cynops pyrrhogaster* [54, 55], the Chinese soft-shelled turtle *Pelodiscus sinensis* [56], the Japanese jungle crow *Corvus macrorhynchos* [57], the American crow *Corvus brachyrhynchos* [58], and the European starling *Sturnus vulgaris* [59]. The second group of species includes those cases in which testis regression is associated with apoptosis, but no conclusive data are reported showing that apoptosis is indeed the cause of germ-cell depletion. In some cases, the highest incidence of apoptosis is observed in the already inactive testis, after germ-cell depletion had taken place, as in the bullfrog *Rana catesbeiana* [60], the white-footed mouse *Peromyscus leucopus* [13, 35], the hare *Lepus europaeus* [14, 61], and the guinea pig *Cavia porcellus* [62]. In other instances, a slightly higher incidence of apoptosis is detected in the inactive testis, but the transition period has not been studied, as in the Syrian hamster *Mesocricetus auratus* [12, 63]. Also in this species, chronic treatment with diethylstilbestrol, a stilbene estrogen acting as an agonist of estradiol-17J3, drastically reduces both FSH and testosterone, leading to a subsequent highly significant surge (10–50-fold) in germ-cell apoptosis, which may explain the germinative-epithelium depletion [64]. However, this severe experimental situation does not reflect the natural conditions of seasonal testis regression in this species. In the Djungarian hamster *Phodopus sungorus*, the method used to quantify the incidence of apoptosis does not ascertain whether the 5-fold increase observed was high enough to explain testis regression by itself. The third group of species includes those for which conclusive evidence has shown that apoptosis is not the cause of testis regression, as in the roe deer *Capreolus capreolus* [15] and the Iberian mole *T. occidentalis* [16]. Accordingly, apoptosis could be considered the main testis-regression effector in birds and maybe also in reptiles and amphibians (more species need to be studied in these taxa), but not in mammals, where the apoptosis paradigm is not fully supported. For the first time, we report here that live germ-cell desquamation is the main testis-regression effector in a mammal, the mole, suggesting that it could also operate in other mammalian species in which apoptosis was definitively ruled out or considered not convincing as an alternative process. Although the number of mammalian species studied is still greatly insufficient, it is noteworthy that the mammals included in the second group belong to the superorder Euarchontoglires, whereas the two species included in the third group belong to the superorder Laurasiateria (also considered a cohort or a magnorder), suggesting a possible phylogenetic origin for the differences pointed out here. Hence, we conclude that data from some previously studied species should be reevaluated and additional seasonal breeding mammals should be studied to elucidate this question.

ACKNOWLEDGMENT

We thank Mr. David Nesbitt for revising the English style of the manuscript.

REFERENCES

1. Zhengwei Y, Wreford NG, De Kretser DM. A quantitative study of spermatogenesis in the developing rat testis. Biol Reprod 1990; 43: 629–635.
2. McLachlan RI, Wreford NG, Robertson DM, de Kretser DM. Hormonal control of spermatogenesis. Trends Endocrinol Metab 1995; 6:95–101.
3. Porkka-Heiskanen T, Khoshaba N, Scarbrough K, Urban JH, Vitaterna MH, Levine JE, Turek FW, Horton TH. Rapid photoperiod-induced increase in detectable GnRH mRNA-containing cells in Siberian hamster. Am J Physiol 1997; 273:R2032–R2039.
4. Russell LD, Clermont Y. Degeneration of germ cells in normal, hypophysectomized and hormone treated hypophysectomized rats. Anat Rec 1977; 187:347–366.
5. Dym M, Fawcett DW. The blood-testis barrier in the rat and the physiological compartmentation of the seminiferous epithelium. Biol Reprod 1970; 3:308–326.
6. Pelletier RM, Byers SW. The blood-testis barrier and Sertoli cell junctions: structural considerations. Microsc Res Tech 1992; 20:3–33.
7. Pelletier RM, Okawara Y, Vitale ML, Anderson JM. Differential distribution of the tight-junction-associated protein ZO-1 isoforms alpha+ and alpha– in guinea pig Sertoli cells: a possible association with F-actin and G-actin. Biol Reprod 1997; 57:367–376.
8. Cheng CY, Mruk DD. An intracellular trafficking pathway in the seminiferous epithelium regulating spermatogenesis: a biochemical and molecular perspective. Crit Rev Biochem Mol Biol 2009; 44:245–263.
9. O'Donnell L, McLachlan RI, Wreford NG, de Kretser DM, Robertson DM. Testosterone withdrawal promotes stage-specific detachment of round spermatids from the rat seminiferous epithelium. Biol Reprod 1996; 55:895–901.
10. Yan HHN, Mruk DD, Lee WM, Cheng CY. Blood-testis barrier dynamics are regulated by testosterone and cytokines via their differential effects on the kinetics of protein endocytosis and recycling in Sertoli cells. FASEB J 2008; 22:1945–1959.
11. Furuta I, Porkka-Heiskanen T, Scarbrough K, Tapanainen J, Turek FW, Hsueh AJ. Photoperiod regulates testis cell apoptosis in Djungarian hamsters. Biol Reprod 1994; 51:1315–1321.
12. Morales E, Pastor LM, Ferrer C, Zuasti A, Pallarés J, Horn R, Calvo A, Santamaría L, Canteras M. Proliferation and apoptosis in the seminiferous epithelium of photoinhibited Syrian hamsters (*Mesocricetus auratus*). Int J Androl 2002; 25:281–287.
13. Young KA, Zirkin BR, Nelson RJ. Short photoperiods evoke testicular apoptosis in white-footed mice (*Peromyscus leucopus*). Endocrinology 1999; 140:3133–3139.
14. Strbenc M, Fazarinc G, Bavdek SV, Pogacnik A. Apoptosis and proliferation during seasonal testis regression in the brown hare (*Lepus europaeus* L.). Anat Histol Embryol 2003; 32:48–53.
15. Blottner S, Schön J, Roelants H. Apoptosis is not the cause of seasonal testicular involution in roe deer. Cell Tissue Res 2007; 327:615–624.
16. Dadhich RK, Real FM, Zurita F, Barrionuevo FJ, Burgos M, Jiménez R. Role of apoptosis and cell proliferation in the testicular dynamics of seasonal breeding mammals: a study in the Iberian mole, *Talpa occidentalis*. Biol Reprod 2010; 83:83–91.
17. Jiménez R, Burgos M, Caballero L, Díaz de la Guardia R. Sex reversal in a

wild population of *Talpa occidentalis* (Insectivora, Mammalia). Genet Res 1988; 52:135–140.
18. Jiménez R, Burgos M, Sánchez A, Sinclair AH, Alarcón FJ, Marín JJ, Ortega E, Díaz de la Guardia R. Fertile females of the mole *Talpa occidentalis* are phenotypic intersexes with ovotestes. Development 1993; 118:1303–1311.
19. Barrionuevo FJ, Zurita F, Burgos M, Jiménez R. Testis-like development of gonads in female moles. New insights on mammalian gonad organogenesis. Dev Biol 2004; 268:39–52.
20. Carmona FD, Lupiáñez DG, Real FM, Burgos M, Zurita F, Jiménez R. SOX9 is not required for the cellular events of testicular organogenesis in XX mole ovotestes. J Exp Zool B Mol Dev Evol 2009;312:734–748.
21. Sánchez A, Bullejos M, Burgos M, Hera C, Stamatopoulos C, Díaz de la Guardia R, Jiménez R. Females of four mole species of genus *Talpa* (insectivora, mammalia) are true hermaphrodites with ovotestes. Mol Reprod Dev 1996; 44:289–294.
22. Rubenstein NM, Cunha GR, Wang YZ, Campbell KL, Conley AJ, Catania KC, Glickman SE, Place NJ. Variation in ovarian morphology in four species of New World moles with a peniform clitoris. Reproduction 2003; 126:713–719.
23. Carmona FD, Motokawa M, Tokita M, Tsuchiya K, Jiménez R, Sánchez-Villagra MR. The evolution of female mole ovotestes evidences high plasticity of mammalian gonad development. J Exp Zool B Mol Dev Evol 2008; 310:259–266.
24. Carmona FD, Lupiáñez DG, Martín J-E, Burgos M, Jiménez R, Zurita F. The spatio-temporal pattern of testis organogenesis in mammals—insights from the mole. Int J Dev Biol 2009; 53:1035–1044.
25. Jiménez R, Burgos M, Sánchez A, Díaz de la Guardia R. The reproductive cycle of *Talpa occidentalis* in the Southeastern Iberian Peninsula. Acta Theriol 1990; 35:165–169.
26. Jiménez R, Alarcón FJ, Sánchez A, Burgos M, De La Guardia RD. Ovotestis variability in young and adult females of the mole *Talpa occidentalis* (Insectivora, Mammalia). J Exp Zool 1996; 274:130–137.
27. Meng J, Holdcraft RW, Shima JE, Griswold MD, Braun RE. Androgens regulate the permeability of the blood-testis barrier. Proc Natl Acad Sci U S A 2005; 102:16696–16700.
28. Dadhich RK, Barrionuevo FJ, Lupiañez DG, Real FM, Burgos M, Jiménez R. Expression of genes controlling testicular development in adult testis of the seasonally breeding iberian mole. Sex Dev 2011; 5:77–88.
29. Gow A, Southwood CM, Li JS, Pariali M, Riordan GP, Brodie SE, Danias J, Bronstein JM, Kachar B, Lazzarini RA. CNS myelin and Sertoli cell tight junction strands are absent in Osp/claudin-11 null mice. Cell 1999; 99:649–659.
30. Pelletier R-M. The blood-testis barrier: the junctional permeability, the proteins and the lipids. Prog Histochem Cytochem 2011; 46:49–127.
31. Sánchez A, Stamatopoulos C, Redi CA. Descriptive kinetics of the seminiferous epithelium cycle and genome size in the mole *Talpa occidentalis* (Insectivora). J Exp Zool 1995; 273:51–58.
32. Batias C, Defamie N, Lablack A, Thepot D, Fenichel P, Segretain D, Pointis G. Modified expression of testicular gap-junction connexin 43 during normal spermatogenic cycle and in altered spermatogenesis. Cell Tissue Res 1999; 298:113–121.
33. Mruk DD, Cheng CY. Sertoli-Sertoli and Sertoli-germ cell interactions and their significance in germ cell movement in the seminiferous epithelium during spermatogenesis. Endocr Rev 2004; 25:747–806.
34. Li MWM, Mruk DD, Lee WM, Cheng CY. Cytokines and junction restructuring events during spermatogenesis in the testis: an emerging concept of regulation. Cytokine Growth Factor Rev 2009; 20:329–338.
35. Young KA, Nelson RJ. Mediation of seasonal testicular regression by apoptosis. Reproduction 2001; 122:677–685.
36. Kotula-Balak M, Hejmej A, Lydka M, Cierpich A, Bilinska B. Detection of aromatase, androgen, and estrogen receptors in bank vole spermatozoa. Theriogenology 2012; 78:385–392.
37. Pastor LM, Zuasti A, Ferrer C, Bernal-Mañas CM, Morales E, Beltrán-Frutos E, Seco-Rovira V. Proliferation and apoptosis in aged and photoregressed mammalian seminiferous epithelium, with particular attention to rodents and humans. Reprod Domest Anim 2011; 46:155–164.
38. Blottner S, Schoen J. Minimal activity in both proliferation and apoptosis of interstitial cells indicates seasonally persisting Leydig cell population in roe deer. Cell Tissue Res 2005; 321:473–478.
39. Muñoz EM, Fogal T, Dominguez S, Scardapane L, Piezzi RS. Ultrastructural and morphometric study of the Sertoli cell of the viscacha (*Lagostomus maximus maximus*) during the annual reproductive cycle. Anat Rec 2001; 262:176–185.
40. Vogl AW, Vaid KS, Guttman JA. The Sertoli cell cytoskeleton. Adv Exp Med Biol 2008; 636:186–211.
41. Mruk DD, Cheng CY. Tight junctions in the testis: new perspectives. Philos Trans R Soc Lond B Biol Sci 2010; 365:1621–1635.
42. Mruk DD, Silvestrini B, Cheng CY. Anchoring junctions as drug targets: role in contraceptive development. Pharmacol Rev 2008; 60:146–180.
43. Yan HHN, Mruk DD, Lee WM, Cheng CY. Cross-talk between tight and anchoring junctions—lesson from the testis. Adv Exp Med Biol 2008; 636:234–254.
44. Kopera IA, Bilinska B, Cheng CY, Mruk DD. Sertoli-germ cell junctions in the testis: a review of recent data. Philos Trans R Soc Lond B Biol Sci 2010; 365:1593–1605.
45. Holthöfer B, Windoffer R, Troyanovsky S, Leube RE. Structure and function of desmosomes. Int Rev Cytol 2007; 264:65–163.
46. Hedger MP. Immunophysiology and pathology of inflammation in the testis and epididymis. J Androl 2011; 32:625–640.
47. Tarulli GA, Meachem SJ, Schlatt S, Stanton PG. Regulation of testicular tight junctions by gonadotrophins in the adult Djungarian hamster in vivo. Reproduction 2008; 135:867–877.
48. McCabe MJ, Tarulli GA, Meachem SJ, Robertson DM, Smooker PM, Stanton PG. Gonadotropins regulate rat testicular tight junctions in vivo. Endocrinology 2010; 151:2911–2922.
49. Meng J, Greenlee AR, Taub CJ, Braun RE. Sertoli cell-specific deletion of the androgen receptor compromises testicular immune privilege in mice. Biol Reprod 2011; 85:254–260.
50. Gye MC. Changes in the expression of claudins and transepithelial electrical resistance of mouse Sertoli cells by Leydig cell coculture. Int J Androl 2003; 26:271–278.
51. Florin A, Maire M, Bozec A, Hellani A, Chater S, Bars R, Chuzel F, Benahmed M. Androgens and postmeiotic germ cells regulate claudin-11 expression in rat Sertoli cells. Endocrinology 2005; 146:1532–1540.
52. Kaitu'u-Lino TJ, Sluka P, Foo CFH, Stanton PG. Claudin-11 expression and localisation is regulated by androgens in rat Sertoli cells in vitro. Reproduction 2007; 133:1169–1179.
53. Xia W, Wong CH, Lee NPY, Lee WM, Cheng CY. Disruption of Sertoli-germ cell adhesion function in the seminiferous epithelium of the rat testis can be limited to adherens junctions without affecting the blood-testis barrier integrity: an in vivo study using an androgen suppression model. J Cell Physiol 2005; 205:141–157.
54. Yazawa T, Yamamoto K, Kikuyama S, Abé SI. Elevation of plasma prolactin concentrations by low temperature is the cause of spermatogonial cell death in the newt, *Cynops pyrrhogaster*. Gen Comp Endocrinol 1999; 113:302–311.
55. Yazawa T, Yamamoto T, Abé S. Prolactin induces apoptosis in the penultimate spermatogonial stage of the testes in Japanese red-bellied newt (*Cynops pyrrhogaster*). Endocrinology 2000; 141:2027–2032.
56. Zhang L, Han X-K, Qi Y-Y, Liu Y, Chen Q-S. Seasonal effects on apoptosis and proliferation of germ cells in the testes of the Chinese soft-shelled turtle, *Pelodiscus sinensis*. Theriogenology 2008; 69:1148–1158.
57. Islam MN, Tsukahara N, Sugita S. Apoptosis-mediated seasonal testicular regression in the Japanese Jungle crow (*Corvus macrorhynchos*). Theriogenology 2012; 77:1854–1865.
58. Jenkins LK, Ross WL, Young KA. Increases in apoptosis and declines in Bcl-XL protein characterise testicular regression in American crows (*Corvus brachyrhynchos*). Reprod Fertil Dev 2007; 19:461–469.
59. Young KA, Ball GF, Nelson RJ. Photoperiod-induced testicular apoptosis in European starlings (*Sturnus vulgaris*). Biol Reprod 2001; 64:706–713.
60. Sasso-Cerri E, Cerri PS, Freymüller E, Miraglia SM. Apoptosis during the seasonal spermatogenic cycle of *Rana catesbeiana*. J Anat 2006; 209: 21–29.
61. Strbenc M, Bavdek SV. Apoptosis and proliferation in the testes of the brown hare (*Lepus europaeus*) under the influence of photoperiod. Pflugers Arch 2001; 442:R161–R162.
62. Hingst O, Blottner S. Quantification of apoptosis (programmed cell death) in mammalian testis by DNA-fragmentation ELISA. Theriogenology 1995; 44:313–319.
63. Morales E, Ferrer C, Zuasti A, Garcia-Borron JC, Canteras M, Pastor LM. Apoptosis and molecular pathways in the seminiferous epithelium of aged and photoinhibited Syrian hamsters (*Mesocricetus auratus*). J Androl 2007; 28:123–135.
64. Nonclercq D, Reverse D, Toubeau G, Beckers JF, Sulon J, Laurent G, Zanen J, Heuson-Stiennon JA. In situ demonstration of germinal cell apoptosis during diethylstilbestrol-induced testis regression in adult male Syrian hamsters. Biol Reprod 1996; 55:1368–1376.